

NJC

Accepted Manuscript



This is an *Accepted Manuscript*, which has been through the Royal Society of Chemistry peer review process and has been accepted for publication.

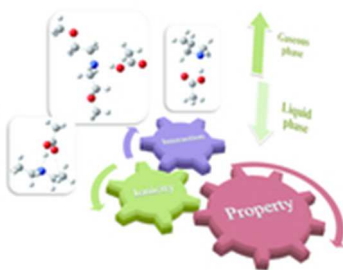
Accepted Manuscripts are published online shortly after acceptance, before technical editing, formatting and proof reading. Using this free service, authors can make their results available to the community, in citable form, before we publish the edited article. We will replace this *Accepted Manuscript* with the edited and formatted *Advance Article* as soon as it is available.

You can find more information about *Accepted Manuscripts* in the [Information for Authors](#).

Please note that technical editing may introduce minor changes to the text and/or graphics, which may alter content. The journal's standard [Terms & Conditions](#) and the [Ethical guidelines](#) still apply. In no event shall the Royal Society of Chemistry be held responsible for any errors or omissions in this *Accepted Manuscript* or any consequences arising from the use of any information it contains.



www.rsc.org/njc



15x12mm (300 x 300 DPI)

Cite this: DOI: 10.1039/c0xx00000x

www.rsc.org/xxxxxx

PAPER

Ionicity in acetate-based protic ionic liquids: evidences for both liquid and gaseous phases†

Xiaofu Sun^a, Shuangyue Liu^b, Asim Khan^c, Chuan Zhao^c, Chuanyu Yan^a and Tiancheng Mu^{a*}

Received (in XXX, XXX) Xth XXXXXXXXXX 20XX, Accepted Xth XXXXXXXXXX 20XX

DOI: 10.1039/b000000x

Low ionicity at high temperatures has been detected for a series of acetate-based protic ionic liquids (PILs), which form neutral components as a result of back proton transfer through an equilibrium shift. By utilising temperature dependence of ¹⁵N NMR, neutral and ionised species are observed. In the meantime, ¹⁵N NMR and Attenuated Total Reflection Fourier Transform Infra Red (ATR-FTIR) spectra indicate that the strength of directional hydrogen bonds is weakened at high temperatures, and ions are apt to form aggregation rather than precursor molecule. *In situ* FT-IR and gas chromatography-electron ionization mass spectrometry (GC-EI-MS) investigations show that the acetate-based PILs exist as both precursor molecule and ion pairs in gaseous phase. Theoretical FT-IR vibrational modes analysis, potential energy surface profile and Atom in Molecular (AIM) analysis of the PILs have been utilized to reveal the essential bonding information, which provide a guide for further application of the PILs.

1. Introduction

Protic ionic liquids (PILs) are an important subclass of ionic liquids (ILs) with many useful properties,¹⁻⁴ and have emerged as a new kind of material⁵⁻⁸ for applications such as fuel cells,⁹⁻¹⁰ chromatography,¹¹ catalytic materials,¹² organic synthesis¹³ and biomass extraction.¹⁴ Based on the Walden plot, many PILs formed by the equimolar mixing of a Brønsted acid to a Brønsted base can be categorized as “poor ILs”.¹⁵ The majority of PILs have non-negligible vapor pressures, but their beneficial properties can potentially outweigh negative properties for certain applications. It is known that the physicochemical properties of PILs can be tailored to applications by adjusting the strength, shape, and size of the constituent acids and bases. The key property that distinguishes PILs from aprotic ionic liquids (AILs) is that proton can transfer from Brønsted acids to the Brønsted bases directly, leading to the presence of proton-donor and proton-acceptor sites, which can be used to build up a unique hydrogen bond network.¹⁶⁻¹⁷ As the cation and anion in each system form more than one hydrogen bonds, all ions together build up dense and cooperative hydrogen bond networks and bi-continuous nanostructures. The presence of these flipping over of hydrogen bond of PILs is thought to promote the aggregation of amphiphilic molecules,¹⁸ which can be attributed to the fast and incomplete proton transfer between the Brønsted acid to the Brønsted base. Therefore, unlike AILs, PILs contain some neutral species, including the aggregation of ions and retro-transfer of proton from cation to anion, along with ions species in the system.

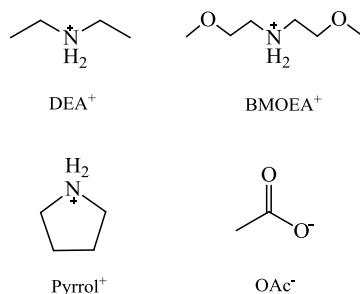
What is the exact composition of PIL systems, true ILs or liquid mixture? Some recent works have argued that the equilibrium of proton-transfer should lie at least 99% towards the ionic species for the mixture to be considered a pure IL.¹⁹⁻²⁰ Thus, ionicity

refers to the fraction of ionic species present in a medium, and is one of the most crucial parameters for characterization of PILs.²¹⁻²²

Aqueous pK_a values for the precursor Brønsted acids and bases have been employed to provide an estimate on how complete proton transfer is, and a large ΔpK_a (pK_a(base) - pK_a(acid)) is usually suggestive of good proton transfer. The investigations by Angell et al.²³ indicated that PILs with ΔpK_a > 8 have nearly ideal Walden behavior. Since ΔpK_a is the driving force shifting the equilibrium toward ionic state,²⁴ ionicity depends on the change in ΔpK_a. It makes many PILs fall into the category of poorly ionised acid-based mixtures or other multi-component mixtures. Special emphasis has been given to the ionicity and other physical and chemical properties.²⁵⁻²⁷ Various techniques such as 1D or 2D NMR,²⁸ IR spectroscopy,²⁰ Walden plot,²¹ changes in thermal properties as a function of stoichiometry, and the ratio of molar conductivities Λ_{imp}/Λ_{NMR} (determined by electrochemical impedance spectroscopy and pulse-field-gradient spin-echo NMR, respectively)²⁹ have been employed for a qualitative measure of the ionic nature of PILs. However, a practical and accurate method for controlling the ionicity and different species in PILs is highly desired.

In this work, the ionicity of three acetate-based PILs (Scheme 1), diethylammonium acetate ([DEA]OAc), bis-(2-methoxyethyl)-ammonium acetate ([BMOEA]OAc) and pyrrolidinium acetate ([Pyrrol]OAc), have been systematically investigated in both the liquid and gaseous phase using a series of methods. These PILs exhibit interesting electrochemical properties for applications as electrolytes.³⁰⁻³¹ The thermal stability and polarity of these PILs have been measured and their ionicity discussed. In particular, all of them are secondary amines, which have a labile proton on the nitrogen centre that can engage in additional hydrogen bonds, thus further promoting the proton transfer. We attempt to describe

the relationship between PILs composition or properties and the atomistic mechanism via the proton motion. ATR-FTIR spectra and ^{15}N NMR spectroscopy are used to detect the composition of PILs in liquid phase, while *in situ* FT-IR and GC-EI-MS are used to obtain the composition of PILs in gaseous phase. The density functional theory (DFT) calculations are carried out to analysis the FT-IR vibrational modes and the potential energy surface profile of PILs. Furthermore, AIM analysis is also performed to further reveal the character of hydrogen bonds among the N-H-O in acetate-based PILs.



Scheme 1 Structures and abbreviations of the cations and the anions of PILs being investigated in this work.

2. Experimental

2.1 Synthesis of the PILs

The PILs were prepared according to the procedure described previously.³⁰⁻³² Briefly, the starting reagents were purified, dried and handled under inert atmosphere. The equimolar neat Brønsted acids as well as Brønsted bases were then added into a round-bottom flask simultaneously while stirred vigorously in acetone-dry ice bath to dissipate the exothermic reaction heat. The prepared PILs samples are highly pure, as confirmed by ^1H NMR and ^{13}C NMR (Bruker AM 400 MHz spectrometer). The water contents of these PILs were determined to be below 100 ppm by Karl-Fischer titration.

2.2 Thermal stability analysis of PILs

Isothermal gravimetric analysis of PILs was carried out using thermogravimetric apparatus (Q50, TA Instruments). In a typical experiment, 8-10 mg of PIL was loaded into the crucible (platinum, 100 μl) under N_2 atmosphere (the sample purge flow rate of $\text{N}_2 = 5 \text{ ml/min}$).

2.3 Polarity measurement of PILs

Nile Red was purchased from J&K Chemical Limited. The stock solution was prepared in menthol and then 200 μl of this solution was added to a quartz cuvette (1.0 \times 0.1 \times 4.5 cm) containing another 200 μl PILs. The quartz cuvette was placed in vacuum to remove the solvent at 40 $^\circ\text{C}$ and then immediately measured with UV-visible spectrophotometer (Carry 5.0, Varian) at room temperature to obtain λ_{max} . Triplicates of each sample were always measured.

2.4 ATR-FTIR spectra measurement of PILs

ATR-FTIR spectroscopy was implemented to investigate the species composition in liquid phase of the acetate-based PILs. The experiments were carried out using a Prestige-21 FT-IR spectrometer (Shimadzu, Japan) using a single reflection ATR cell. Acquisition was accomplished in the DTGS detector mode using an accumulation rate of 40 scans at a resolution of 4 cm^{-1} at

room temperature ($\sim 25 \text{ }^\circ\text{C}$) in the spectral range of 400 to 4600 cm^{-1} . Triplicates of each sample were measured.

2.5 ^{15}N NMR spectra of PILs

^{15}N NMR spectra of samples were acquired with a Bruker Avance 600 MHz spectrometer. The ^{15}N chemical shifts were referred to external saturated aq. NH_4Cl in a co-axial capillary. The PILs were measured as neat liquids using co-axial capillary containing 1 wt% sodium 3-(trimethylsilyl) propionic acid- d_4 acid (TSP) in D_2O solution as a lock solution.

2.6 The viscosity and ionic conductivity measurement of PILs

The values of viscosity of PILs were recorded from 0 to 50 $^\circ\text{C}$ in 5 $^\circ\text{C}$ increments on an automated micro-viscometer by Anton Paar (AMVn). The ionic conductivity of PILs were measured by employing the complex impedance method at the corresponding temperature. The measurements are carried out using a Solartron immediate response analyzer in the frequency range between 0.1 Hz and 1 Hz. A locally designed conductivity cell made from two platinum wires was applied for experiments and the cell constant was determined by calibration using a 0.01 mol/L KCl aqueous solution.

2.7 *In-situ* FT-IR measurement of PILs

The *in-situ* FT-IR characterization was carried out using the Fourier transform infrared spectrometer (Nicolet 6700, thermo, USA), a stainless steel cell with ZnSe windows and a vacuum system. Each PIL was put into the cell and heated up to every corresponding temperature by 5 $^\circ\text{C}/\text{min}$ stepwise. Then the FT-IR spectra of the vapor phase of them were collected at each temperature and triplicates of each sample were measured.

2.8 EI-MS spectra of PILs

The EI-MS spectra of the PILs were recorded with SHIMADZU GC-MS-QP2010 instrument and collected at 70 eV. All the samples were dissolved in chloroform.

2.9 Computational methods

The geometries of the reactants, transition states and products were fully optimized at B3LYP/6-311++G(d,p) basis set. The interaction energy (ΔE) including the basis set superposition errors (BSSE) correction using the counterpoise (CP) method was estimated. AIM analysis was performed using B3LYP/6-311++G(d,p) basis set to confirm the existence of hydrogen bond. All the DFT calculations were carried out with Gaussian 03 package.³³

3. Results and discussion

3.1 Thermal stability of the acetate-based PILs

It is generally accepted that a typical ILs possess high thermal stability and non-measurable vapour pressure.³⁴ However, the acetate-based PILs investigated in this study exhibit different features compared to traditional AILs. To evaluate the thermal properties and long-term stability of these PILs, including decomposition and vaporization, the isothermal thermogravimetric measurements are performed at 40 $^\circ\text{C}$ for 4 h (Fig. 1A). The acetate-based PILs show significant weight loss with the increasing of temperature. Among these PILs, [BMOEA]OAc has the poorest stability, which merely has about 30 wt% remained after 4 h. [DEA]OAc shows a weight loss of about 10 % in 4 h at 25 $^\circ\text{C}$ and under N_2 atmosphere (the sample purge flow rate of $\text{N}_2 = 5 \text{ mL/min}$), which reaches to about 50 % at 70 $^\circ\text{C}$ (Fig. 1B). It should be noted that the pseudo-first-order

reaction kinetic model is suitable for [DEA]OAc, while [Pyrrol]OAc and [BMOEA]OAc obviously follow zero-order kinetics. The weight loss can be viewed as the retro-transfer of the proton from cation to anion due to the nonvolatility of single ion. It follows the proton-transfer mechanism that could facilitate vaporization of PILs as neutral species.³⁵ It can be approximately considered to be equal to the formation rate from ion-pair state to the molecular state, following proton transfer order of [BMOEA]OAc > [Pyrrol]OAc > [DEA]OAc.

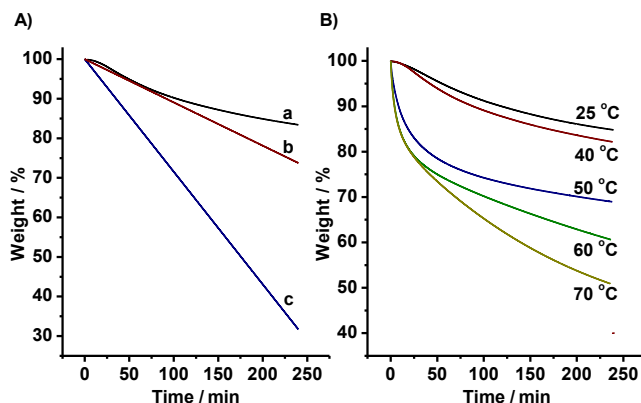


Fig. 1 Time-dependent isothermal TGA for, A) different PILs: [DEA]OAc (a), [Pyrrol]OAc (b) and [BMOEA]OAc (c) at 40 °C and, B) [DEA]OAc at different temperature for 4 h under an N₂ atmosphere.

To investigate the correlation between the structure and the thermal stability of these PILs, we measured the polarity of the PILs using Nile Red, a positively solvatochromic dye.³⁶ The wavelength of its absorption maximum (λ_{max}) has a red shift when dissolved in the acetate-based PILs: [DEA]OAc ($\lambda_{\text{max}} = 569$ nm) > [Pyrrol]OAc ($\lambda_{\text{max}} = 555$ nm) > [BMOEA]OAc ($\lambda_{\text{max}} = 550$ nm), indicating a polarity order of [DEA]OAc > [Pyrrol]OAc > [BMOEA]OAc. Since the dipole-dipole interaction between polar molecules causes greater attachment and is stronger than the dispersion force in less polar molecules, the thermal stability of these PILs shows the same order as their polarity.

What causes the weight loss of the PILs, vaporization or decomposition, and how to make the composition change from the existing species? Generally, thermal instability of PILs can be explained via the ionicity. To prove this concept, the composition species of both the liquid and gaseous phase of these acetate-based PILs were investigated using a range of methods at different temperatures.

ATR-FTIR spectra analysis in the liquid phase

Firstly, ATR-FTIR spectra of the PILs and their precursors are recorded at room temperature. The main assignments of the vibrational mode of the PILs and their precursors are listed in Table S1 and Table S2. Taking [DEA]OAc as an example, the vibrational frequency and mode of some functional groups has changed significantly compared with the precursors DEA and HAc. The symmetric stretching vibration and asymmetric stretching vibration of C-N-C in [DEA]OAc exhibit a red-shift in frequency, indicating the bonding energy becomes smaller in this PIL. The stretching vibration frequency in 3284 cm⁻¹ and 3361 cm⁻¹ of N-H has a blue shift, while the vibrational frequency of N-H in DEA is 3280 cm⁻¹. The absorption band between 1747

cm⁻¹ and 1669 cm⁻¹ in the acetic acid spectrum is associated mainly with the C=O bond asymmetric stretching vibration,³⁷ while [DEA]OAc does not show any absorbance at this frequency interval, suggesting that no acetic acid molecule exists in [DEA]OAc. The stretching vibration frequency of C-O bond and C=O bond in the acetic acid is observed at 1226 cm⁻¹ and 1711 cm⁻¹, respectively. In the formation of [DEA]OAc, the proton transfer makes the bonding energy of C-O and C=O average, leading to the blue-shift in symmetric stretching vibration frequency (1333 cm⁻¹) and the red-shift in asymmetric stretching vibration frequency (1631 cm⁻¹) (Fig. S1). Interestingly, a small peak is found at 2195 cm⁻¹ in the ATR-IR spectrum for [DEA]OAc, which shows a significant red shift when a small amount of water (< 1000 ppm) is added to accelerate the proton transfer. Different from the common red-shift hydrogen bonds, the IR intensity doesn't increase correspondingly. The peak is attributed to the vibration absorption peak of N-H-O, which is formed via fast labile proton hopping between the N atom in amine and the O atom in acetate.

Similar trend in the change of the vibrational modes also has been observed for [BMOEA]OAc and [Pyrrol]OAc. The symmetric stretching vibration and asymmetric stretching vibration of C-N-C in the cations show a red-shift, while the stretching vibration frequencies of N-H show blue shifts. In the acetate anions, the blue-shift in symmetric stretching vibration frequency and the red-shift in asymmetric stretching vibration frequency can be observed. These results indicate the strong interactions exist between the cations and anions of the PILs. By comparison, [BMOEA]OAc has the least shift in the IR spectra, taking the N-H bond as an example, which implies this PIL has a large ionicity.

¹⁵N NMR spectroscopy with different temperature

In order to further clarify the composition of the PILs, ¹⁵N NMR spectroscopy is used to determine the nitrogen substitution at the exchange site, and to distinguish between protonated and non-protonated nitrogen in the liquid phase of the PILs. Due to the poor natural abundance as well as low and negative magnetogyric ratio of ¹⁵N nucleus,³⁸ the ionization by ¹⁵N NMR are determined using neat PILs samples, which could be acquired in a reasonable time and provided information on the intrinsic properties of the PILs.³² For [DEA]OAc, two ¹⁵N resonances are obtained (Fig. 2A) at a temperature range from 10 °C to 50 °C with 10 °C intervals. At 10 °C, the protonated [DEA] molecule showed ¹⁵N chemical shift at 24.646 ppm. The upfield shift of the other ¹⁵N at 23.981 ppm was attributed to ion aggregates, which are formed by hydrogen bond interaction between [DEA] cation and [OAc] anion through the N-H-O bond. It can be seen in Table 1 that both chemical shifts in the NMR spectra decrease, at different magnitudes, with the increasing of temperature. So the difference values of two ¹⁵N resonances increase linearly with the increasing of temperature. (Fig. 2B) Coincidentally, the ratio of integral relative peak area of both ¹⁵N resonances has the same trend. The result indicates that the ionicity of [DEA]OAc decreases with increasing temperature, owing to the retro-transfer of proton through shift of equilibrium,³⁹ and the fact that neutralization by the precursors is exothermic. Hence, successive breaking of hydrogen bonds with temperature can explain the relatively low ionicity and other characteristic properties of [DEA]OAc.

Weakening the strength of directional hydrogen bonds may induce formation of ion aggregates.³⁹ The ions in PIL are not condensed and the remaining interaction is the non-directional, non-localized and low-temperature-dependent Coulombic force.⁴⁰ So, ion aggregates can be formed in [DEA]OAc as neutral components by the retro-transfer of proton to reduce the ionicity of [DEA]OAc.

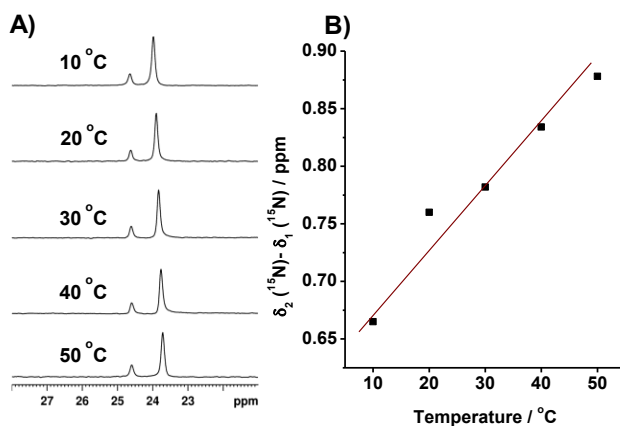


Fig. 2 ¹⁵N NMR spectra of [DEA]OAc at different temperature.

Table 1 ¹⁵N chemical shifts in [DEA]OAc measured as neat liquid at different temperature.

Entry	Temperature (°C)	δ_1 (¹⁵ N) (ppm)	δ_2 (¹⁵ N) (ppm)	$\Delta[\delta(^{15}\text{N})]^a$ (ppm)	The ratio of S_1/S_2^b
1	10	23.981	24.646	0.665	3.61
2	20	23.902	24.622	0.760	3.89
3	30	23.832	24.614	0.782	4.16
4	40	23.765	24.599	0.834	4.43
5	50	23.715	24.593	0.878	4.70

^a $\Delta[\delta(^{15}\text{N})] = \delta_2(^{15}\text{N}) - \delta_1(^{15}\text{N})$
^b S_1 and S_2 represent the integral relative peak area of two ¹⁵N resonances in each ¹⁵N NMR spectra.

In contrast comparison, only the isotropic signal of ¹⁵N is obtained for [BMOEA]OAc (Fig. 3A) and [Pyrrol]OAc (Fig. 4A), which is an average of protonated and molecular bases. It indicates that faster intermolecular proton exchange and a weaker hydrogen bonds formed between the ion aggregates in these two PILs, comparing to [DEA]OAc. The ¹⁵N NMR spectra of these PILs have an upfield shift with increasing temperature. It reveals that the strength of hydrogen bonds decreased and the content of ion aggregates increased at high temperature, which results in a low ionicity. Fig. 3B and Fig. 4B show that the average ¹⁵N chemical shifts change linearly with the temperature and is more prominent in [BMOEA]OAc than in [Pyrrol]OAc with the increasing temperature. (Fig. S2) Since [BMOEA] has a relatively large size, the stabilization of hydrogen bond in

[BMOEA]OAc needs more energy, which results in relatively easy formation of both ion aggregates and neutral components (the absorption of about 1700 cm⁻¹) easily, and consequently a poorer thermal stability than [Pyrrol]OAc. The NMR line width of [BMOEA]OAc and [Pyrrol]OAc decreased slightly with the increasing of temperature, suggesting that the molecular relaxation time changes with temperature. The relative wide line width at low temperature possibly implies that the proton-exchange rate decreases with increasing temperature, and the stronger interaction with the dipole among ions may be existed.

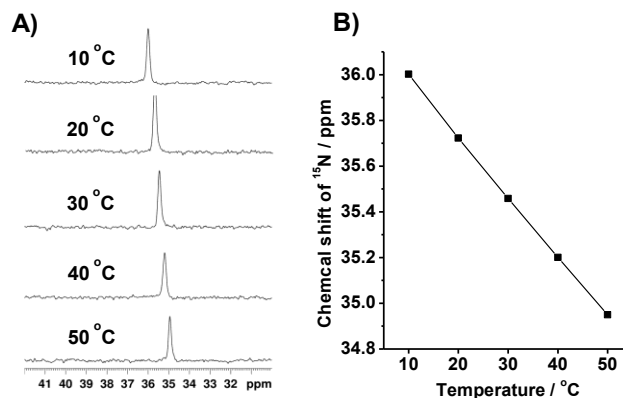


Fig. 3 ¹⁵N NMR spectra of [BMOEA]OAc at different temperature.

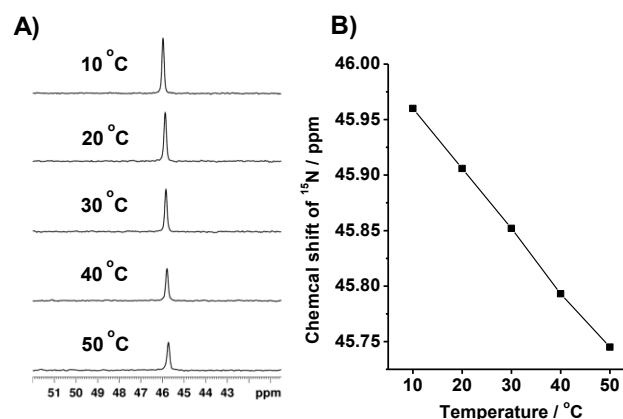


Fig. 4 ¹⁵N NMR spectra of [Pyrrol]OAc at different temperature.

Due to the complex composition, hydrogen bonds are a hallmark of these acetate-based PILs as donor and acceptor groups are formed on the ions during synthesis via proton transfer.⁴¹⁻⁴² The strength of hydrogen bonds depends on temperature and structure as well as the interaction strength of acid and amine. The ionicity of the PILs in the liquid phase thus can be correlated with the strength of hydrogen bonds. The decrease in ionicity of the PILs at high temperatures can mainly be attributed to the formation of ion aggregates. Here, Scheme S1 could be used to describe the situation and the main forces involved in the liquid phase of PILs.

The Walden Plot is further applied to verify the order of ionicity of the acetate-based PILs. Fig. S3 and Fig. S4 in the ESI shows the viscosities and ionic conductivities of the present acetate-based PILs as a function of temperature. Based on the 5 Walden plot in Fig. S5 and the concept of Angell *et al.*,¹⁸ these PILs are poor ionic liquids with incomplete proton transfer, indicating the order of the ionicity: [BMOEA]OAc > [Pyrrol]OAc > [DEA]OAc. Generally, a large ionicity close to unity implies weak interionic interactions. The result is also in 10 accordance with that obtained via ATR-FTIR and ¹⁵N NMR in this study. This can also be related to ΔpK_a of these PILs as the ΔpK_a value of [Pyrrol]OAc (6.52) is slightly higher than that of [DEA]OAc (6.24).

Investigation of the ionicity and interaction in the gaseous phase

Under certain conditions some ILs including PILs can be distilled and many ILs can decompose into their precursor species or the fragments.^{34, 43-44} In addition to the verification of the presence of 20 both ion-pairs and molecular aggregates in the PILs in liquid phase, we also investigate the states of the acetate-based PILs in gaseous phase using *in situ* FT-IR method.⁴⁵

Fig. 5 shows the *in situ* gaseous FT-IR spectrum of [BMOEA]OAc at different temperatures, which has the poorest thermal stability among the three acetate-based PILs. The 25 absorption peaks at 1716 and 1635 cm^{-1} when [BMOEA]OAc is distilled at 160 °C in vacuum, are assigned to C=O bond stretching vibration of the molecular species and ionic species respectively. These results are in good agreement with the liquid phase spectra of [BMOEA]OAc.

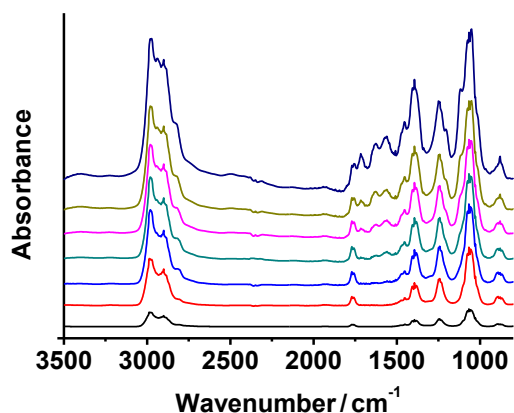


Fig. 5 The *in situ* gas FT-IR spectra of [BMOEA]OAc at different temperature (from bottom to top: 40 °C, 80 °C, 120 °C, 140 °C, 160 °C, 200 °C and 250 °C).

It is noted that the neutral molecules and ion species can only be probed at high temperatures, which implies that proton needs 35 to span the low-energy-barrier to form neutral molecules and then evaporate from the condensed phase. Obviously, the absorbance intensity of the two peaks increases with the increasing temperature. It indicates that [BMOEA]OAc may evaporate via neutral molecules, similar to AILs⁴⁶, and then the ion pairs can be 40 obtained by the transfer of the proton from the acid to base. Therefore, OAc⁻ anion and acetic acid molecule exist in the

gaseous phase of [BMOEA]OAc simultaneously at high temperature. Similar phenomenon are also found for [DEA]OAc (Fig. S6) and [Pyrrol]OAc (Fig. S7). Therefore, from the 45 investigation of gaseous structures of the PILs by *in situ* FT-IR, it can be concluded that the proton transfer occurs in the process of vaporization, and the molecular and ionic aggregates coexist in the gaseous phase of the PILs.

We hypothesize that back proton transfer occurs in the system 50 through the equilibrium shift toward neutral components. It can be seen that the experimental values of the frequencies are limited by experimental condition, so the calculated frequency values can be used to analyse the vibrational modes of the PILs. All the PILs have been fully optimized and shown in Fig. 6. From IRC 55 calculation, we obtain a transition state (TS) that has single imaginary frequency. The potential energy surface (PES) profile of the PILs is depicted in Fig. S8, Fig. S9 and Fig. S10, respectively. The associated neutral components are formed by the isolate cations and anions via TS in Fig. 6. The energy of the 60 products, A₁, A₂ and A₃, are 24.93, 17.55 and 3.24 kJ/mol higher than the reactants [DEA]OAc, [BMOEA]OAc and [Pyrrol]OAc, respectively. This is in agreement with the facts that these PILs are less stable than their precursors in our experiments.



Fig. 6 Optimized structures of the interaction between cations and anions in the present acetate-based PILs at B3LYP/6-311++G (d, p).

The assignments of calculated FT-IR wave numbers are also aided by the animation option of Gaussview 3.0 graphical interface for Gaussian programs, which could give a visual 70 presentation of the shape of the vibrational modes (Table S1, Table S3, Table S4 and Table S5). The discrepancy between the observed and calculated frequencies can be ascribed to the fact that the calculations were actually based on a single molecule in the gaseous state rather than in the presence of intermolecular 75 interactions, as recorded for the experimental values. The proton transfer mechanism of these acetate-based PILs from ionic state to TS, which has an imaginary frequency in the IR, then to molecular state is quite consistent. In the process of TS formation, both the bending vibration and stretching vibration (including the 80 symmetric stretching vibration and asymmetric stretching vibration) of C-N-C bond and the stretching vibration of N-H bond are blue-shifted significantly and the bond length becomes shorter, suggesting more compact binding between the atoms. In ionic state, the distance of N-H is longer, leading to weaker 85 interaction with H atom. For acetate anion sp² hybridization is adopted by the C atom in the O-C-O bond and the negative charge can be distributed to two O atoms averagely under the effect of p- π conjugation. When a proton is accepted by the acetate anion, the C=O is broken and forms a single bond, leading

to the red-shift in bending vibration and the symmetric stretching vibration, and the blue-shift in asymmetric stretching vibration. After that, TS is inclined to form the neutral species, which results in the blue-shift in the symmetric stretching vibration and the red-shift in the asymmetric stretching vibration of C-N-C bond. The vibration frequency of N-H is hardly changed in this process. The blue shift occurred in the bending vibration and the stretching vibration of O-C-O, suggesting it is more stable than the TS. An important finding in comparing experimental IR and theoretical calculation is that an equilibrium of proton transfer do exist in the present acetate-based PILs.

Table 2 AIM parameters of N-H-O bonds for the present acetate-based PILs

PILs	$\rho(R)$	$\nabla^2\rho(R)$	H_{BCP}
[DEA]OAc	0.055188	0.09275	-0.006299
[BMOEA]OAc	0.041642	0.09283	-0.009552
[Pyrrol]OAc	0.049588	0.09894	-0.001534

Moreover, in order to further examine the character of hydrogen bonding among the N-H-O, AIM analysis is performed and the results are summarized in Table 2, which identifies a unique line of communication between two chemically interacting nuclei, and provides a unique measure to probe the interaction.⁴⁷⁻⁴⁸ Among them, the topology of the charge density, $\rho(R)$, at a bond critical point (BCP) can be described as the strength of the bond. It can be seen that the $\rho(R)$ of all the PILs are higher than the charge density of traditional hydrogen bonds (0.002-0.04),⁴⁷ which implies the strong hydrogen bond interactions in these PILs. It can also be found that the $\rho(R)$ values of the PILs abide with the order of [DEA]OAc > [Pyrrol]OAc > [BMOEA]OAc, suggesting that the strength of hydrogen bond weakens subsequently in the present acetate-based PILs. We draw the same conclusion that the order of the ionicity of PILs follows [BMOEA]OAc > [Pyrrol]OAc > [DEA]OAc. The Laplacian of the charge density, $\nabla^2\rho(R)$, can be used to determine the character of interaction between atoms. A positive $\nabla^2\rho(R)$ reflects an excess of kinetic energy in a bond, and this is the case that the closed-shell (electrostatic) interactions can be viewed as the main interaction in the PILs. In addition, the energy density of the charge at BCP (H_{BCP}) is more rational for describing the nature of the non-bonded interaction.⁴⁹ The negative values of H_{BCP} indicate that the interactions through covalent bonding also exist in the PIL systems and have a trend of proton transfer.

Furthermore, GC-EI-MS experiments have been carried out to investigate gas phase structures of the acetate-based PILs.⁵⁰ The EI-MS spectra of the PILs (Table 3) show that the peaks corresponding to the ionized base molecules of m/z 73.0, 133.0 and 71.0 can be observed for [DEA]OAc, [BMOEA]OAc and [Pyrrol]OAc, respectively. The ions of m/z 74.0, 134.0 and 72.0 are also present, which stand for the amine cations of three PILs, respectively. From the spectra of [DEA]OAc and [Pyrrol]OAc, the ratios of the ionized status amine in the gas phase are calculated to be 8.58 % and 12.28%, indicating that [DEA]OAc and [Pyrrol]OAc exist mainly as molecule in the gas phase and the weight loss processes predominantly involve the vaporization of the neutral precursor molecules formed by the retro-transfer of

the proton from cation to anion. However, in the case of [BMOEA]OAc, the ratio of ionized and molecular status amine in the gas phase is 50.69 %. The ion peak at m/z 134.0 corresponds to the [BMOEA] cation, which confirms that molecular and ionic aggregates co-exist in the gas phase of [BMOEA]OAc, and indicates that although the PILs can be evaporated in the form of precursor molecular state, it may still have the reaction of proton-transfer ($A + B \rightarrow A^+ + BH^+$) in the gas phase. Therefore, the order of ionicity in the gas phase of the PILs is: [BMOEA]OAc > [Pyrrol]OAc > [DEA]OAc. Due to the polarity order: [DEA]OAc > [Pyrrol]OAc > [BMOEA]OAc, the gas phase structure of PILs depends not only on the types of acid and base, but also the polarity of the molecules. It can be concluded that both discrete anion-cation pairs and neutral molecules exist in the gas phases of these PILs, which is consistent with the results obtained via *in situ* FT-IR and theoretical calculations. In addition, molecular species can dominate in the gas phase in high polarity PILs [DEA]OAc and [Pyrrol]OAc.

Table 3 The chemical structure, the mass-to-charge ratio (m/z) and the relative abundance of neutral base molecule and amine cation of the present acetate-based PILs.

PILs	Chemical structure		m/z (B, BH ⁺)	Relative Abundance		BH ⁺ in Gas Phase (%)
	Neutral Molecule (B)	Cation (BH ⁺)		B	BH ⁺	
[DEA]OAc			73.0, 74.0	100	9.38	8.58
[BMOEA]OAc			133.0, 134.0	100	102.78	50.69
[Pyrrol]OAc			71.0, 72.0	100	14.00	12.28

4. Conclusions

We have provided detailed experimental evidence and theoretical calculations for the species composition in both liquid and gaseous phases of three acetate-based PILs using a combination of methods including ATR-FTIR, ¹⁵N NMR, *in situ* FT-IR, GC-EI-MS and DFT. The absorption band of C=O bond stretching vibration in ATR-FTIR spectra and temperature dependence of ¹⁵N chemical shift indicated that cations, anions and ionic aggregates co-exist in the liquid phase. The strength of the directional hydrogen bonds may weaken and non-directional, non-localized and low-temperature-dependent Coulombic force became the main interaction between the ions, which is to say that the ionicity in the liquid phase of the PILs decreases with the increasing temperature. According to *in situ* FTIR and GC-EI-MS study, all the PILs exist as both precursor molecule and ion pairs in gaseous phase, and the ratio of ionized and molecular status base depends on the type of precursor and the polarity of PILs. The molecular species may dominate in the gaseous phase for high polarity PILs. Importantly, the DFT calculations, including the theoretical FT-IR vibrational modes analysis, the potential energy surface profile and AIM analysis of PILs provide the theoretical support to the experimental results. The present study

provides insight into the behavior of PILs, which could be useful for understanding and designing of novel PILs for a range of applications.

Acknowledgements

This work was funded by the National Natural Science Foundation of China (Grant 21173267), and an Australian Research Council Discovery Grant (DP110102569).

Notes and references

^a Department of Chemistry, Renmin University of China, Beijing 100872, P. R. China. Tel: 8610-62514925, Email : tcmu@chem.ruc.edu.cn

^b School of Chemistry and Chemical Engineering, Qufu Normal University, Qufu 273165, P. R. China

^c School of Chemistry, The University of New South Wales, NSW 2052, Australia

† Electronic Supplementary Information (ESI) available: See DOI: 10.1039/b000000x/

1. T. L. Greaves and C. J. Drummond, *Chem. Rev.*, 2008, **108**, 206-237.
2. J. P. Belieres and C. A. Angell, *J. Phys. Chem. B*, 2007, **111**, 4926-4937.
3. T. L. Greaves, A. Weerawardena, C. Fong, I. Krodkiewska and C. J. Drummond, *J. Phys. Chem. B*, 2006, **110**, 22479-22487.
4. K. Ghandi, *Green Sustainable Chem.*, 2014, **4**, 44-53.
5. M. Treskow, J. Pitawala, S. Arenz, A. Matic and P. Johansson, *J. Phys. Chem. Lett.*, 2012, **3**, 2114-2119.
6. C. Yansheng, Z. Zhida, L. Changping, L. Qingshan, Y. Peifang and U. Welz-Biermann, *Green Chem.*, 2011, **13**, 666-670.
7. D. R. MacFarlane, N. Tachikawa, M. Forsyth, J. M. Pringle, P. C. Howlett, G. D. Elliott, J. H. Davis, M. Watanabe, P. Simon and C. A. Angell, *Energy Environ. Sci.*, 2014, **7**, 232-250.
8. J. Stoimenovski, P. M. Dean, E. I. Izgorodina and D. R. MacFarlane, *Faraday Discuss.*, 2012, **154**, 335-352.
9. B. C. Lin, S. Cheng, L. H. Qiu, F. Yan, S. M. Shang and J. M. Lu, *Chem. Mater.*, 2010, **22**, 1807-1813.
10. U. A. Rana, M. Forsyth, D. R. MacFarlane and J. M. Pringle, *Electrochim. Acta*, 2012, **84**, 213-222.
11. F. Pacholec, H. T. Butler and C. F. Poole, *Anal. Chem.*, 1982, **54**, 1938-1941.
12. J. Snyder, T. Fujita, M. Chen and J. Erlebacher, *Nat. Mater.*, 2010, **9**, 904-907.
13. G. A. Olah, T. Mathew, A. Goepfert, B. Török, I. Bucsí, X.-Y. Li, Q. Wang, E. R. Martinez, P. Batamack and R. Aniszfeld, *J. Am. Chem. Soc.*, 2005, **127**, 5964-5969.
14. E. C. Achinivu, R. M. Howard, G. Li, H. Gracz and W. A. Henderson, *Green Chem.*, 2014, **16**, 1114-1119.
15. K. Ueno, H. Tokuda and M. Watanabe, *Phys. Chem. Chem. Phys.*, 2010, **12**, 1649-1658.
16. K. Fumino, A. Wulf and R. Ludwig, *Angew. Chem. Int. Ed.*, 2009, **48**, 3184-3186.
17. K. Fumino, P. Stange, V. Fossog, R. Hempelmann and R. Ludwig, *Angew. Chem. Int. Ed.*, 2013, **52**, 12439-12442.
18. J. Hunger, T. Sonnleitner, L. Y. Liu, R. Buchner, M. Bonn and H. J. Bakker, *J. Phys. Chem. Lett.*, 2012, **3**, 3034-3038.
19. K. M. Johansson, E. I. Izgorodina, M. Forsyth, D. R. MacFarlane and K. R. Seddon, *Phys. Chem. Chem. Phys.*, 2008, **10**, 2972-2978.

20. B. Nuthakki, T. L. Greaves, I. Krodkiewska, A. Weerawardena, M. I. Burgar, R. J. Mulder and C. J. Drummond, *Aust. J. Chem.*, 2007, **60**, 21-28.
21. D. R. MacFarlane, M. Forsyth, E. I. Izgorodina, A. P. Abbott, G. Annat and K. Fraser, *Phys. Chem. Chem. Phys.*, 2009, **11**, 4962-4967.
22. J. Stoimenovski, E. I. Izgorodina and D. R. MacFarlane, *Phys. Chem. Chem. Phys.*, 2010, **12**, 10341-10347.
23. M. Yoshizawa, W. Xu and C. A. Angell, *J. Am. Chem. Soc.*, 2003, **125**, 15411-15419.
24. M. S. Miran, H. Kinoshita, T. Yasuda, M. A. Susan and M. Watanabe, *Phys. Chem. Chem. Phys.*, 2012, **14**, 5178-5186.
25. R. Hayes, S. Imberti, G. G. Warr and R. Atkin, *Angew. Chem. Int. Ed.*, 2012, **51**, 7468-7471.
26. S. B. Capelo, T. Mendez-Morales, J. Carrete, E. L. Lago, J. Vila, O. Cabeza, J. R. Rodriguez, M. Turmine and L. M. Varela, *J. Phys. Chem. B*, 2012, **116**, 11302-11312.
27. T. L. Greaves, A. Weerawardena, I. Krodkiewska and C. J. Drummond, *J. Phys. Chem. B*, 2008, **112**, 896-905.
28. P. Judeinstein, C. Iojoiu, J. Y. Sanchez and B. Ancian, *J. Phys. Chem. B*, 2008, **112**, 3680-3683.
29. H. Tokuda, S. Tsuzuki, M. A. B. H. Susan, K. Hayamizu and M. Watanabe, *J. Phys. Chem. B*, 2006, **110**, 19593-19600.
30. C. Zhao, A. M. Bond and X. Y. Lu, *Anal. Chem.*, 2012, **84**, 2784-2791.
31. C. Zhao, G. Burrell, A. A. J. Torriero, F. Separovic, N. F. Dunlop, D. R. MacFarlane and A. M. Bond, *J. Phys. Chem. B*, 2008, **112**, 6923-6936.
32. G. L. Burrell, I. M. Burgar, F. Separovic and N. F. Dunlop, *Phys. Chem. Chem. Phys.*, 2010, **12**, 1571-1577.
33. M. J. Frisch, G. W. Trucks, H. B. Schlegel, G. E. Scuseria, M. A. Robb, J. R. Cheeseman, J. A. Montgomery, T. Vreven, K. N. Kudin, J. C. Burant, J. M. Millam, S. S. Iyengar, J. Tomasi, V. Barone, B. Mennucci, M. Cossi, G. Scalmani, N. Rega, G. A. Petersson, H. Nakatsuji, M. Hada, M. Ehara, K. Toyota, R. Fukuda, J. Hasegawa, M. Ishida, T. Nakajima, Y. Honda, O. Kitao, H. Nakai, M. Klene, X. Li, J. E. Knox, H. P. Hratchian, J. B. Cross, V. Bakken, C. Adamo, J. Jaramillo, R. Gomperts, R. E. Stratmann, O. Yazyev, A. J. Austin, R. Cammi, C. Pomelli, J. W. Ochterski, P. Y. Ayala, K. Morokuma, G. A. Voth, P. Salvador, J. J. Dannenberg, V. G. Zakrzewski, S. Dapprich, A. D. Daniels, M. C. Strain, O. Farkas, D. K. Malick, A. D. Rabuck, K. Raghavachari, J. B. Foresman, J. V. Ortiz, Q. Cui, A. G. Baboul, S. Clifford, J. Cioslowski, B. Stefanov, G. Liu, A. Liashenko, P. Piskorz, I. Komaromi, R. L. Martin, D. J. Fox, T. Keith, Al M. A. Laham, C. Y. Peng, A. Nanayakkara, M. Challacombe, P. M. W. Gill, B. Johnson, W. Chen, M. W. Wong, C. Gonzalez, J. A. Pople, Gaussian 03, revision C.02; Gaussian, Inc.: Wallingford, CT, **2004**.
34. M. J. Earle, J. M. Esperança, M. A. Gilea, J. N. C. Lopes, L. P. Rebelo, J. W. Magee, K. R. Seddon and J. A. Widegren, *Nature*, 2006, **439**, 831-834.
35. B. A. D. Neto, L. S. Santos, F. M. Nachtigall, M. N. Eberlin and J. Dupont, *Angew. Chem. Int. Ed.*, 2006, **45**, 7251-7254.
36. Y. Chen, Y. Cao, X. Lu, C. Zhao, C. Yan and T. Mu, *New J. Chem.*, 2013, **37**, 1959-1967.

37. A. B. Pereiro, J. M. M. Araujo, F. S. Oliveira, C. E. S. Bernardes, J. Esperanca, J. N. C. Lopes, I. M. Marrucho and L. P. N. Rebelo, *Chem. Commun.*, 2012, **48**, 3656-3658.
38. A. Lycka, R. Dolecek, P. Simunek and V. Machacek, *Magn. Reson. Chem.*, 2006, **44**, 521-523.
39. M. S. Miran, H. Kinoshita, T. Yasuda, M. Abu Bin, H. Susanz and M. Watanabe, *Chem. Commun.*, 2011, **47**, 12676-12678.
40. K. Fumino, A. Wulf and R. Ludwig, *Angew. Chem. Int. Ed.*, 2008, **47**, 8731-8734.
41. R. Hayes, S. Imberti, G. G. Warr and R. Atkin, *Angew. Chem. Int. Ed.*, 2013.
42. J. Smith, G. B. Webber, G. G. Warr and R. Atkin, *J. Phys. Chem. B*, 2013, **117**, 13930-13935.
43. S. A. Chowdhury, R. Vijayaraghavan and D. MacFarlane, *Green Chem.*, 2010, **12**, 1023-1028.
44. A. E. Rosamilia, C. R. Strauss and J. L. Scott, *Pure Appl. Chem.*, 2007, **79**, 1869-1877.
45. K. Dong, L. D. Zhao, Q. Wang, Y. T. Song and S. J. Zhang, *Phys. Chem. Chem. Phys.*, 2013, **15**, 6034-6040.
46. C. M. Wang, H. M. Luo, H. R. Li and S. Dai, *Phys. Chem. Chem. Phys.*, 2010, **12**, 7246-7250.
47. J. D. Dunitz and A. Gavezzotti, *Angew. Chem. Int. Ed.*, 2005, **44**, 1766-1787.
48. W. D. Arnold and E. Oldfield, *J. Am. Chem. Soc.*, 2000, **122**, 12835-12841.
49. Y. Wang, H. Li and S. Han, *J. Chem. Phys.*, 2006, **124**, 044504.
50. X. Zhu, Y. Wang and H. R. Li, *Phys. Chem. Chem. Phys.*, 2011, **13**, 17445-17448.

30